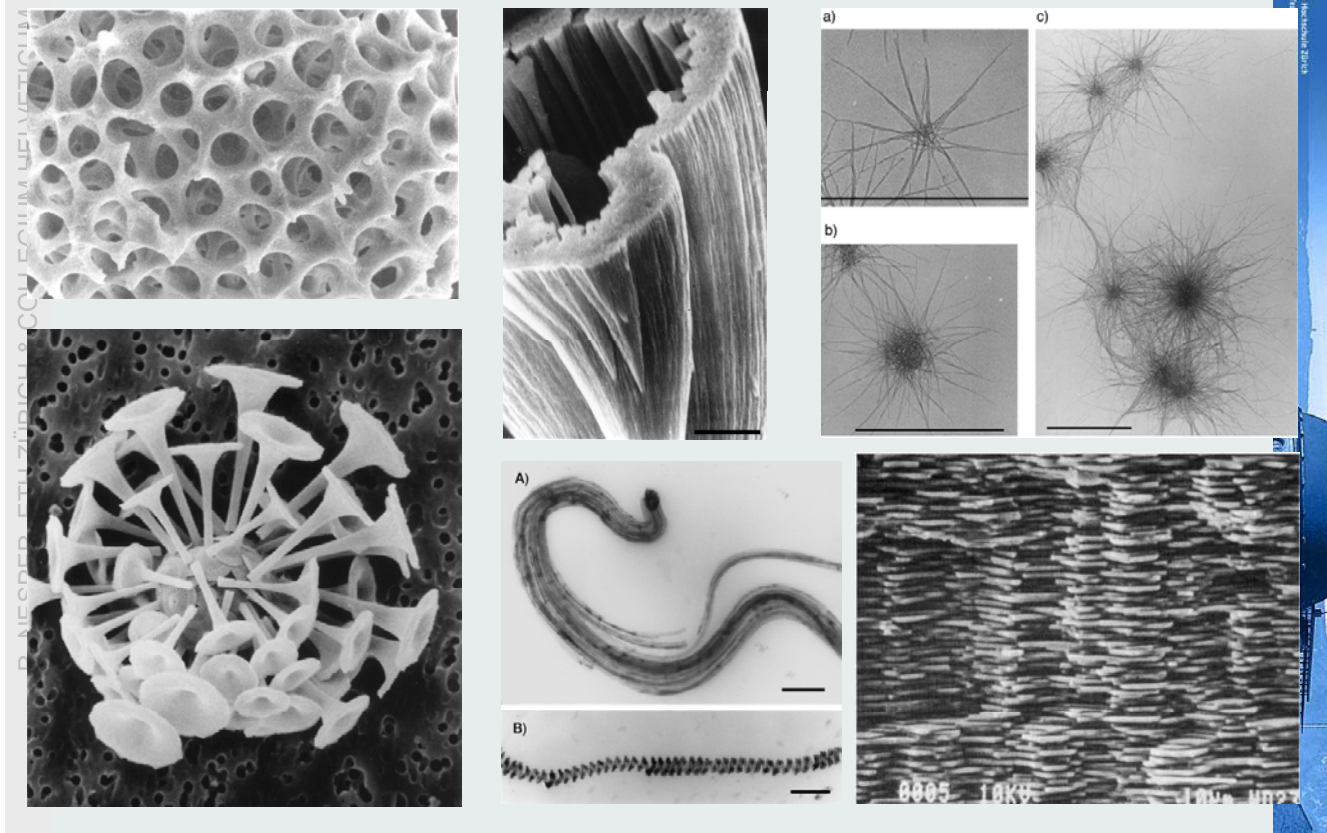


Forms of Minerals in Biology



Function of Minerals in Biology

- protection
- motion
- cutting and grinding
- buoyancy
- optical, magnetic and gravity sensing
- storage.

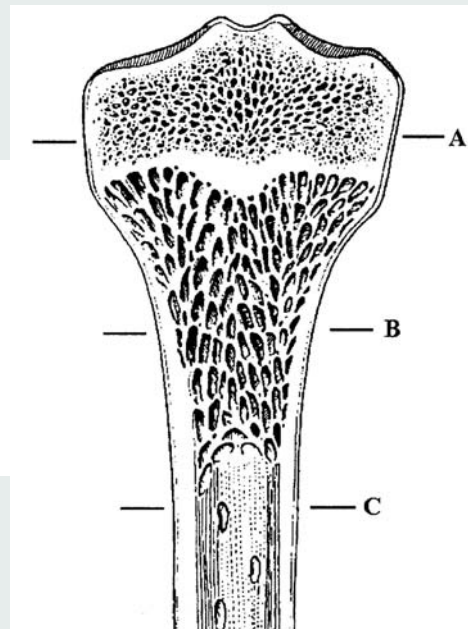


Fig. 2.9 Internal structure of long bone with three different microstructures (A, B and C).

Minerals in Biology

TABLE 11.8 Most Important Biominerals

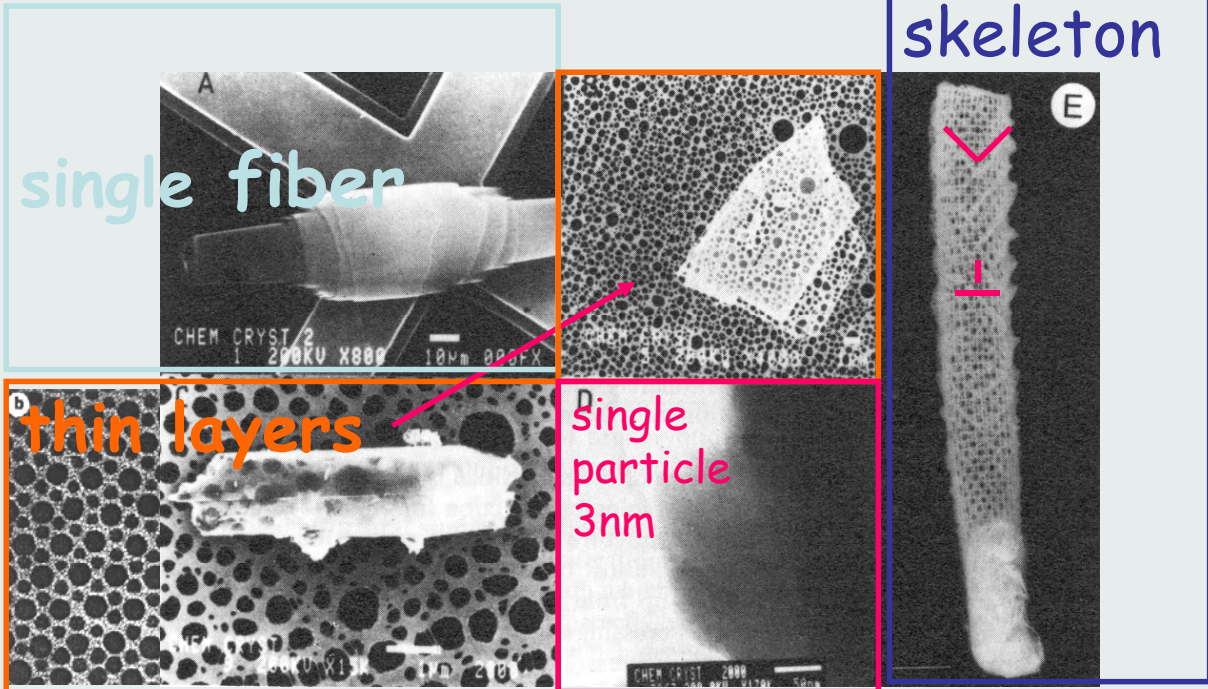
| Chemical Composition | Mineral Phase | Function and Examples |
|--|--|--|
| Calcium carbonate CaCO_3 | Calcite Aragonite Vaterite Amorphous | Exoskeletons (e.g., egg shells, corals, mollusks, sponge spicules) |
| Calcium phosphates $\text{Ca}_{10}(\text{OH})_2(\text{PO}_4)_6$ $\text{Ca}_{10-x}(\text{HPO}_4)_x(\text{PO}_4)_{6-x}(\text{OH})_{2-x}$ $\text{Ca}_{10}\text{F}_2(\text{PO}_4)_6$ $\text{Ca}_2(\text{HPO}_4)_2 \cdot 2\text{H}_2\text{O}$ | Hydroxyapatite (HAP) Defect apatites Fluoroapatite Dicalcium phosphate dihydrate (DCPD) | Endoskeletons (bones and teeth) |
| $\text{Ca}_2(\text{HPO}_4)_2$ | Dicalcium phosphate (DCPA) | |
| $\text{Ca}_8(\text{HPO}_4)_2(\text{PO}_4)_4 \cdot \text{H}_2\text{O}$ | Octacalcium phosphate (OCP) | |
| $\text{Ca}_3(\text{PO}_4)_2$ | β -Tricalcium phosphate (TCP) | |
| Calcium oxalate $\text{Ca}_x\text{C}_2\text{O}_4 \cdot (1 \text{ or } 2)\text{H}_2\text{O}$ | Whewellite Whedelite | Calcium storage and passive deposits in plants calculi of excretory tracts |
| Metal sulfates $\text{CaSO}_4 \cdot 2\text{H}_2\text{O}$ SrSO_4 BaSO_4 | Gypsum Celestite Baryte | Gravity sensors Exoskeletons (acantharia) Gravity sensors |
| Amorphous silica $\text{SiO}_n(\text{OH})_{4-2n}$ | Amorphous (opal) | Defense in plants, diatom valves, sponge spicules, and radiolarian tests |
| Iron oxides Fe_3O_4 | Magnetite | Chiton teeth, magnetic sensors |
| $\alpha, \gamma\text{-Fe(O)OH}$ $5\text{Fe}_2\text{O}_3 \cdot 9\text{H}_2\text{O}$ | Goethite, lepidocrocite Ferrihydrite | Chiton teeth Chiton teeth, iron storage |

Reproducibility of Minerals in Biology

Table 2.3 Chemical composition of calcium phosphate (hydroxyapatite) in human and shark enamel

| Composition (wt%) | Human enamel | Shark enamel |
|--------------------|--------------|--------------|
| Ca^{2+} | 37.55 | 37.26 |
| Na^+ | 0.75 | 0.76 |
| Mg^{2+} | 0.27 | 0.32 |
| PO_4^{3-} | 17.68 | 17.91 |
| CO_3^{2-} | 3.6 | 1.1 |
| F^- | 0.02 | 3.65 |

Silica - deep sea sponge

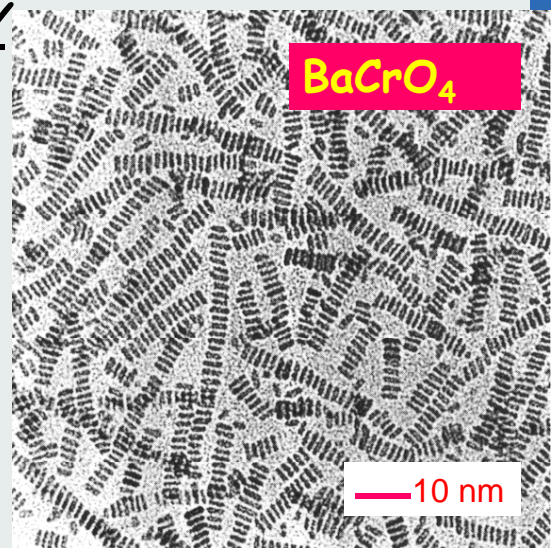
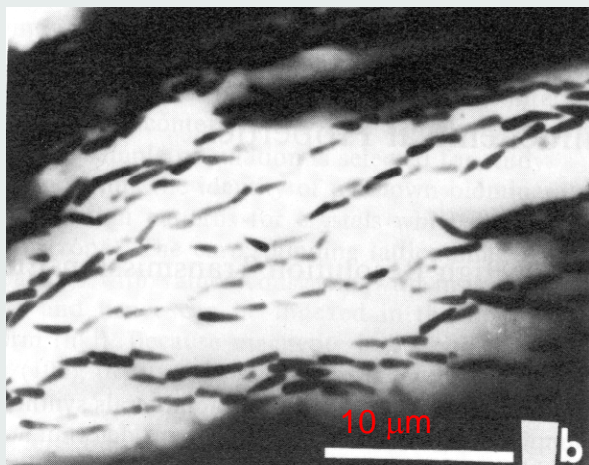


C.C.Perry in S. Mann, J.Webb, R.J.P.Williams, Biominerization, VCH 1989

Advanced Selfassembly

Magnetosomes in algae

S. Mann, R.B. Frankel
in S. Mann, J.Webb,
R.J.P.Williams, Biominerization,
VCH 1989



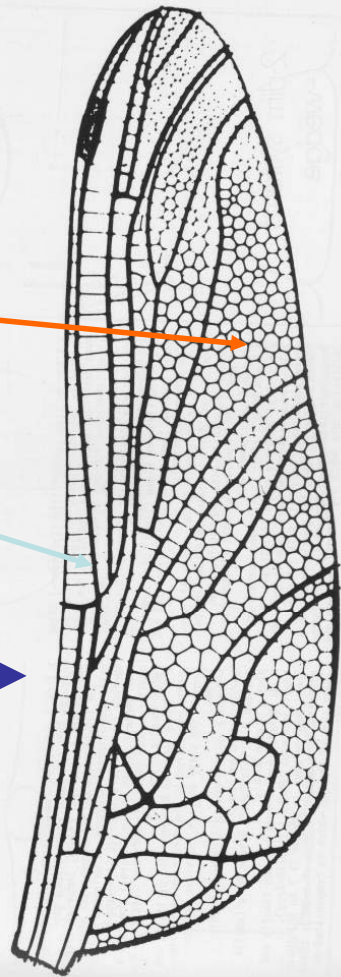
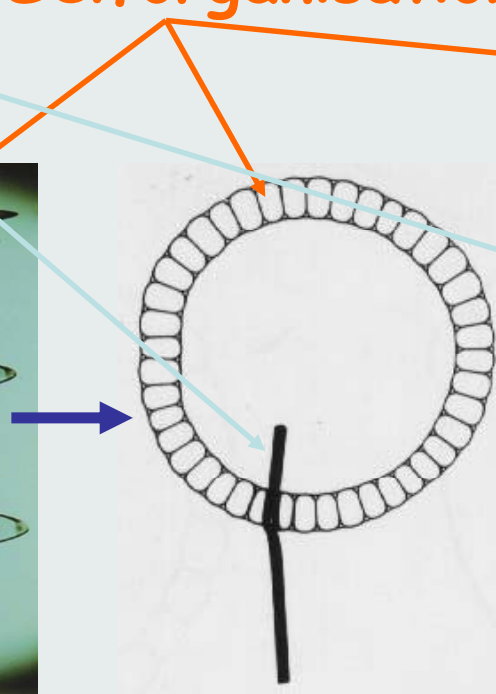
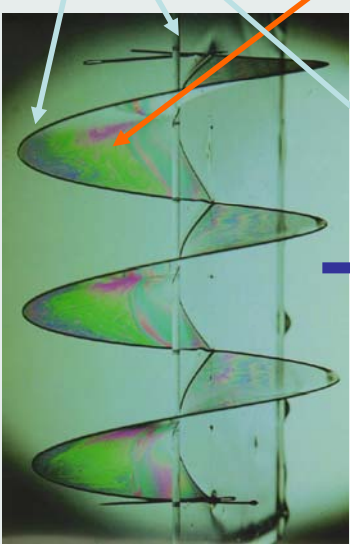
**Coupled synthesis and self-assembly
of nanoparticles to give structures
with controlled organization**

Mei Li*, Heimo Schnablegger† & Stephen Mann*

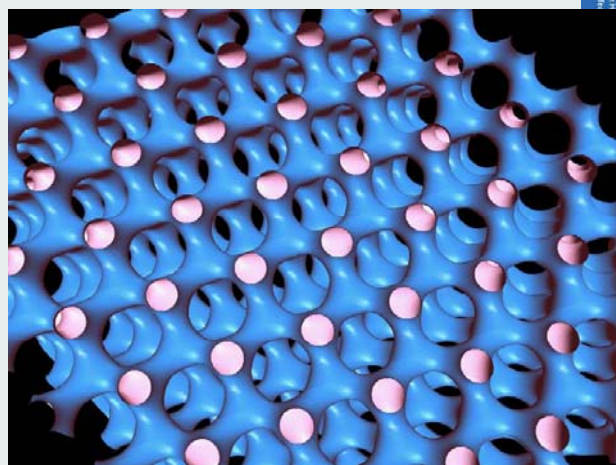
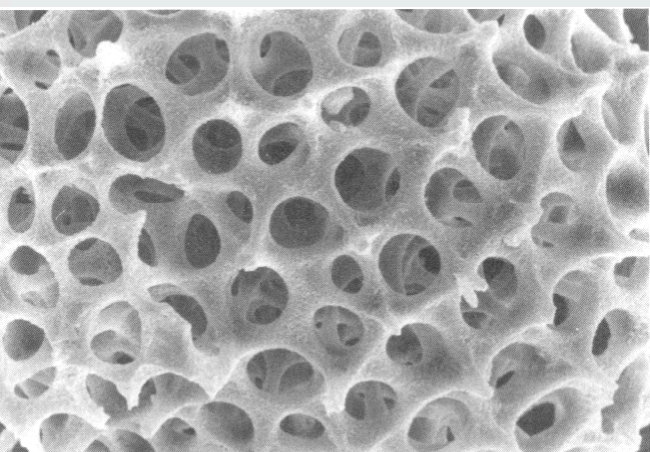
Nature (1999) 402, 393

Bio"mineralization"

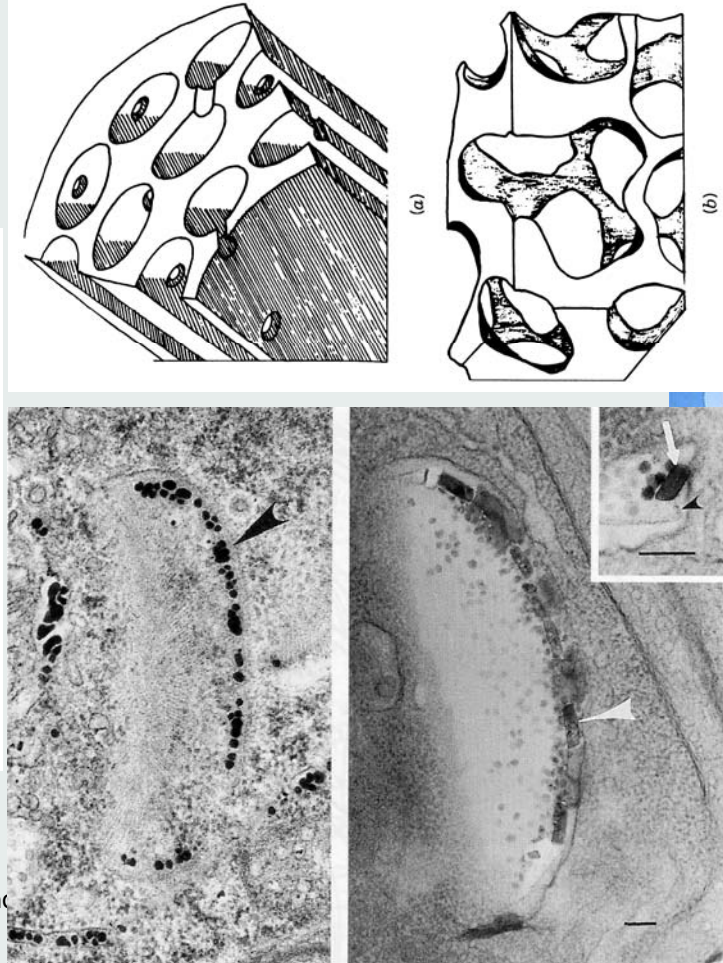
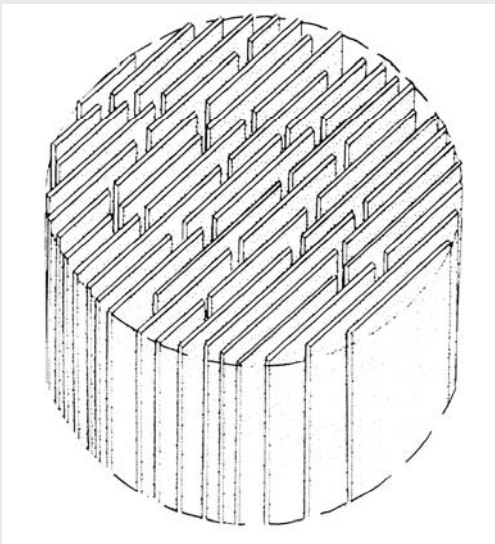
Design + Selforganisation



More Complex Forms of Minerals in Biology



Design of Complex Forms



How is it achieved?

Table 3.2 The main types of biominerization processes

| Process | Control mechanism | Concepts | Properties | Chapter |
|---|-------------------|---|---|---------|
| Precipitation (crystallization) | Chemical | Solubility Supersaturation Nucleation Growth | Solution composition Promotion Inhibition Phase transformation | 4 |
| Boundary-organized biominerization | Spatial | Supramolecular preorganization | Physical boundary Diffusion-limited site Ion transport Size and shape Organization | 5 |
| Organic matrix-mediated biominerization | Structural | Interfacial molecular recognition | Site-directed nucleation Oriented nucleation Supporting framework Mechanical design | 6 |
| Morphogenesis | Morphological | Vectorial regulation | Complex form Time-dependent form Patterning | 7 |
| Biomineral tectonics | Constructional | Multilevel processing | Higher-order assembly Hierarchical structures Integrative building modules Adaptive structures and functions | 8 |

What is achieved ?

- uniform particle sizes
- well-defined structures and compositions
- high levels of spatial organization
- complex morphologies
- controlled aggregation and texture
- preferential crystallographic orientation
- higher-order assembly into hierarchical structures.

What is achieved ?

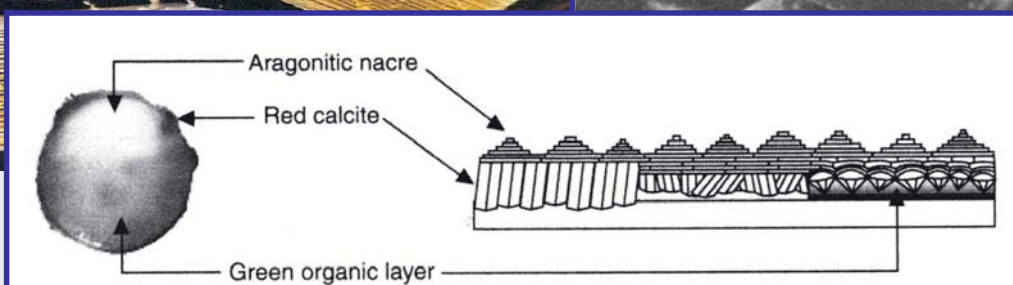
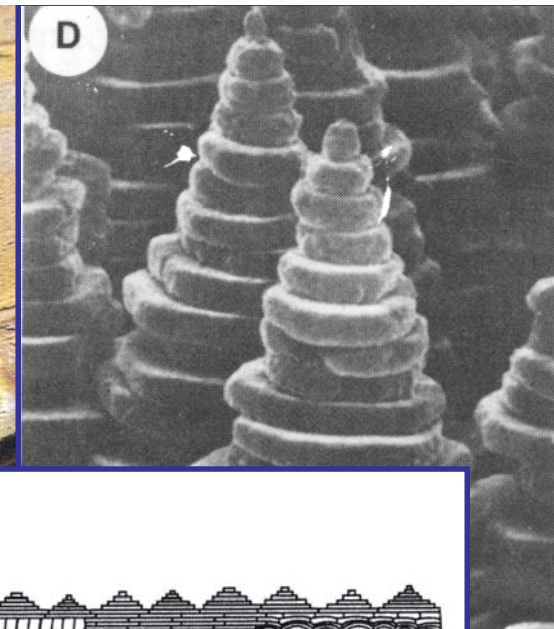
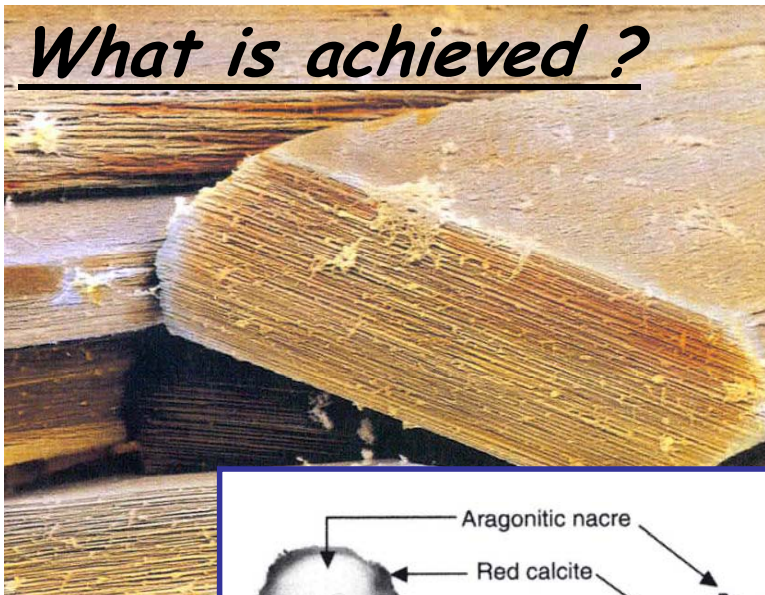


Figure 15.3 A mature flat pearl. The c-axis of the nacre is perpendicular to the paper. The three different regions of the flat pearl are labeled red calcite, aragonitic nacre and green organic layer. The schematic diagram on the right shows the spatial organization of the regions.

Toughness

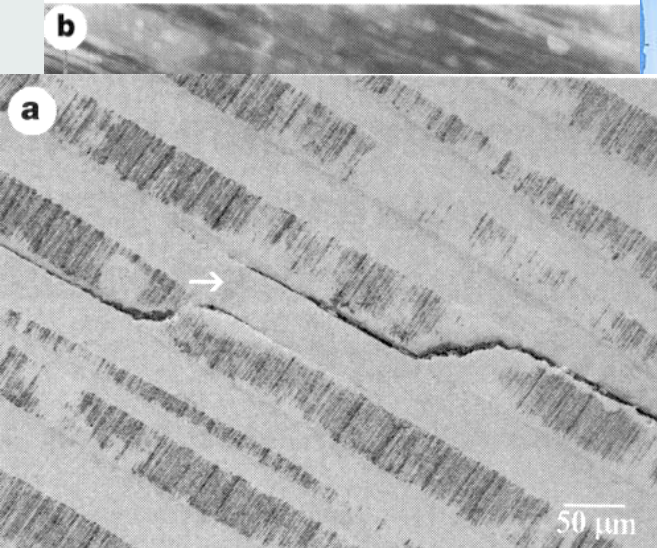
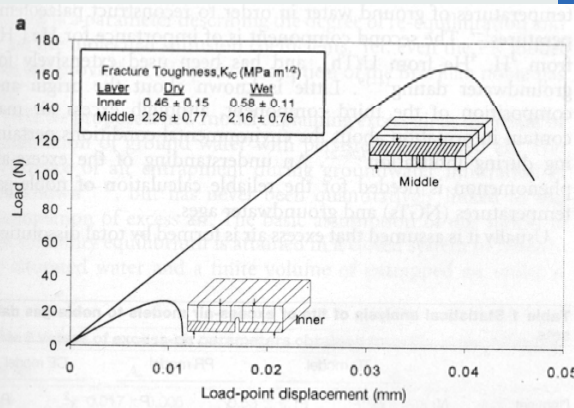
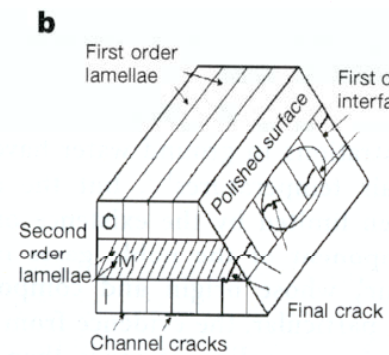
Structural basis for the fracture toughness of the shell of the conch *Strombus gigas*

S. Kamat*, X. Su*, R. Ballarini† & A. H. Heuer*

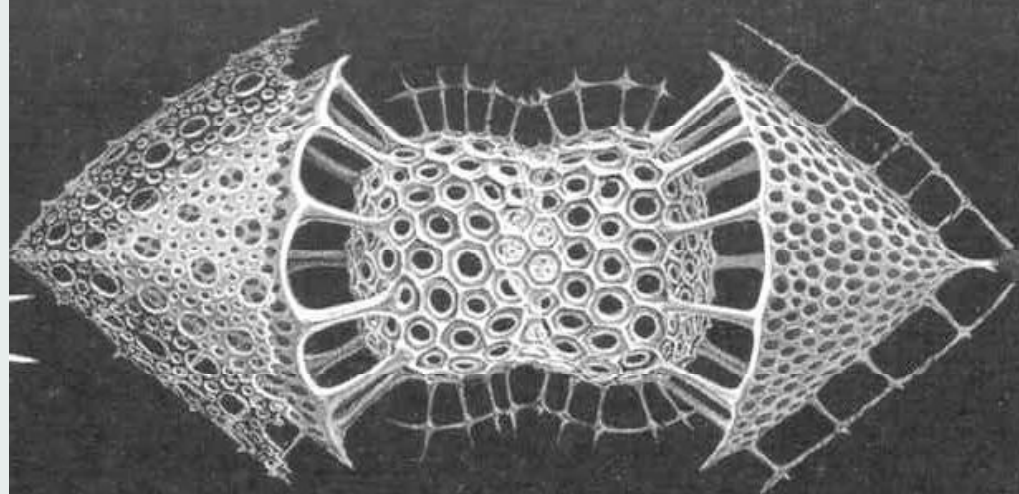
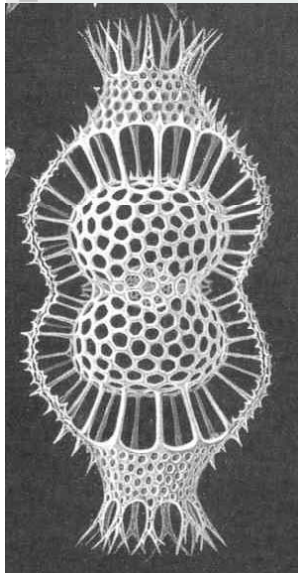
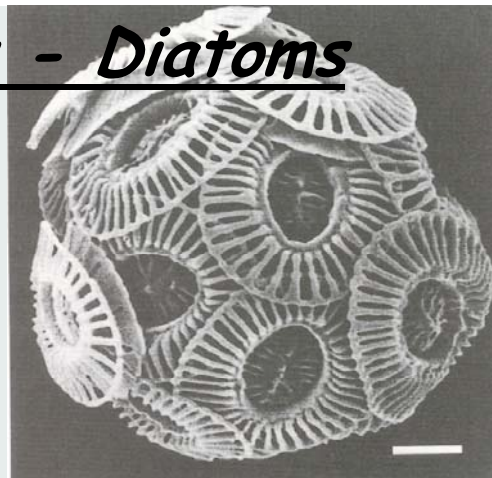
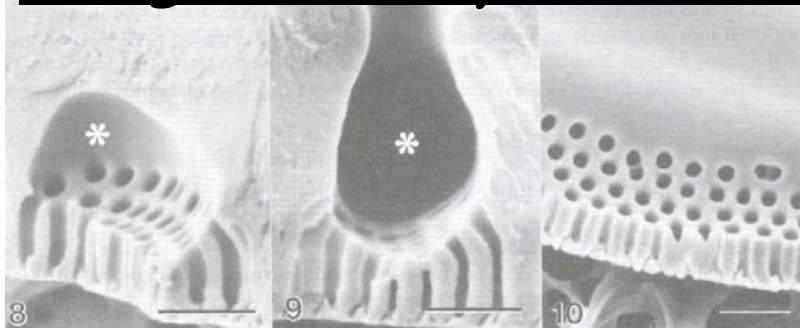
Nature 405 (2000) 1038

ZÜRICH & COLLEGIAL

- Layers : 0.5-2mm
1. Order lamella : 5-60mm
2. Order lamella : 5-30mm
3. Order lamella : 60-130nm



Design of Complex Forms - Diatoms



How is it achieved ?

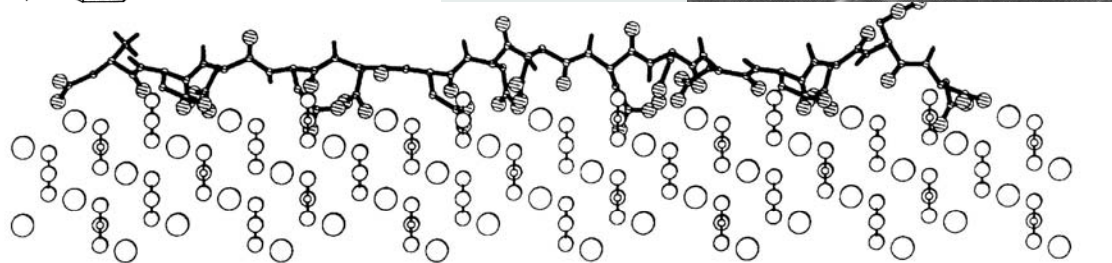
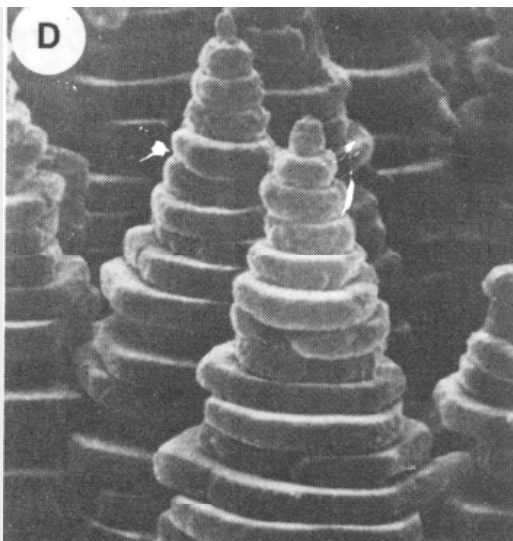
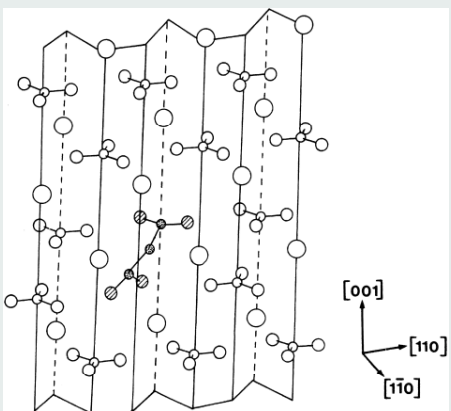
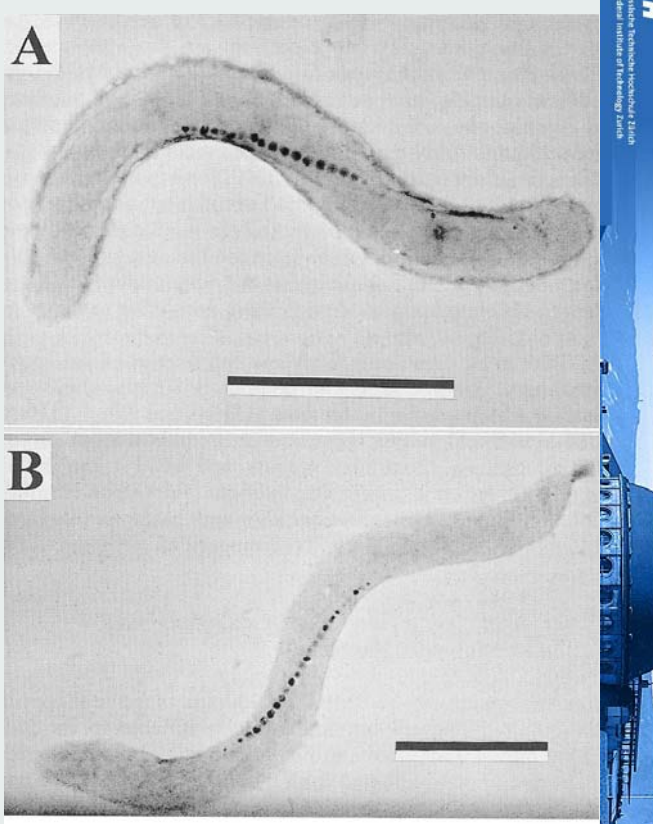


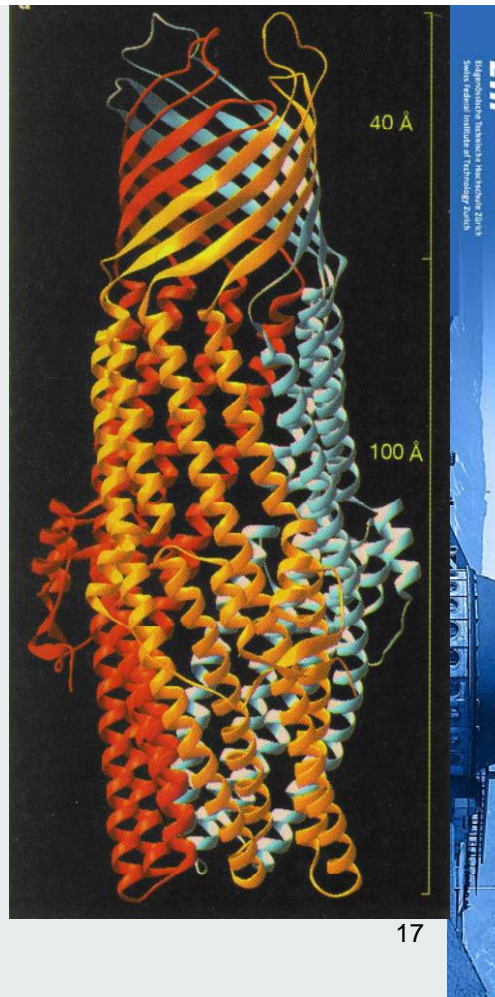
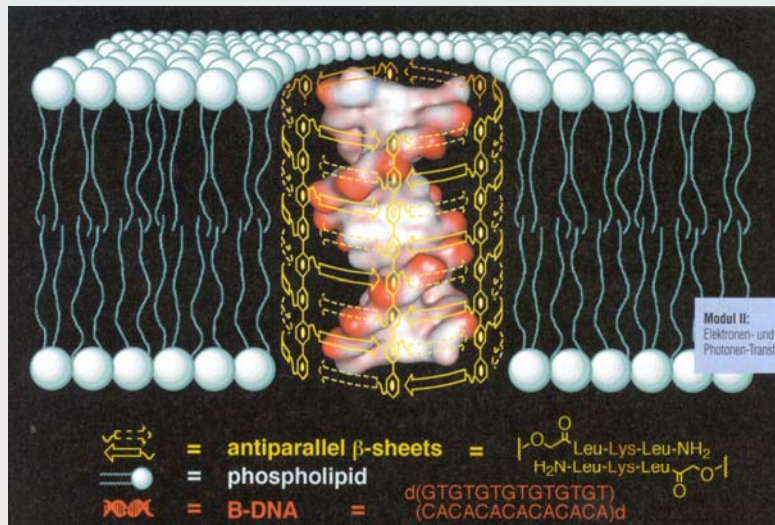
Fig. 4.23 Computer model showing side view of the calcite $\{1\bar{1}0\}$ face with surface-bound polyaspartate ($[Asp]_{11}$).

Control and Function

- chemical
- spatial
- structural
- morphological
- constructional.



Control and Function



Nanochemistry UIO

17

Biodynamic Restoration

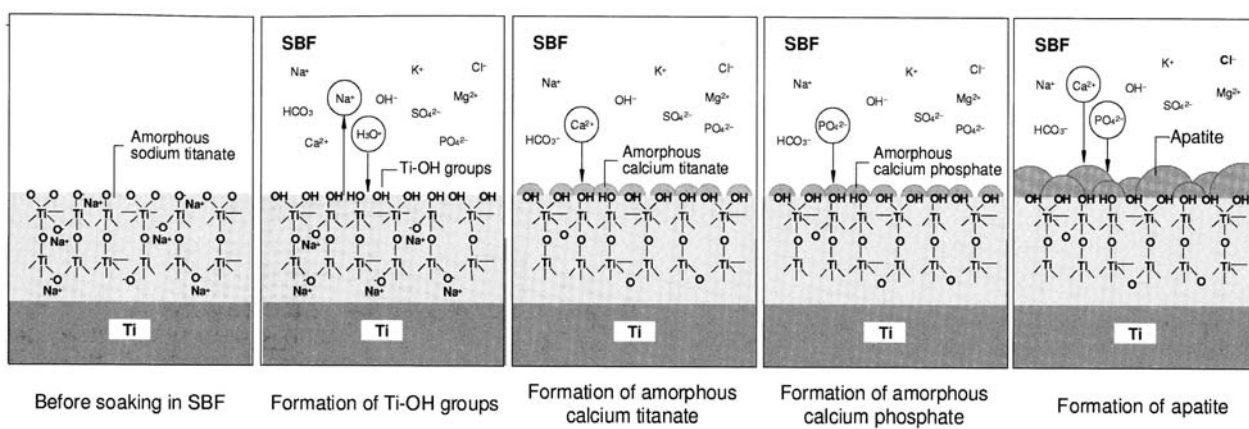


Figure 2. Schematic representation of the mechanism of apatite formation on NaOH-treated Ti metal in simulated body fluid (SBF) (from Reference 10).

Nanochemistry UIO

18

Enamel Formation

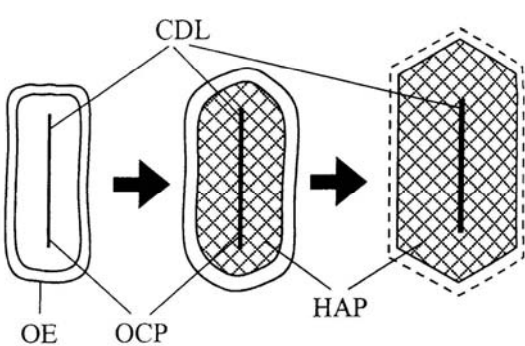
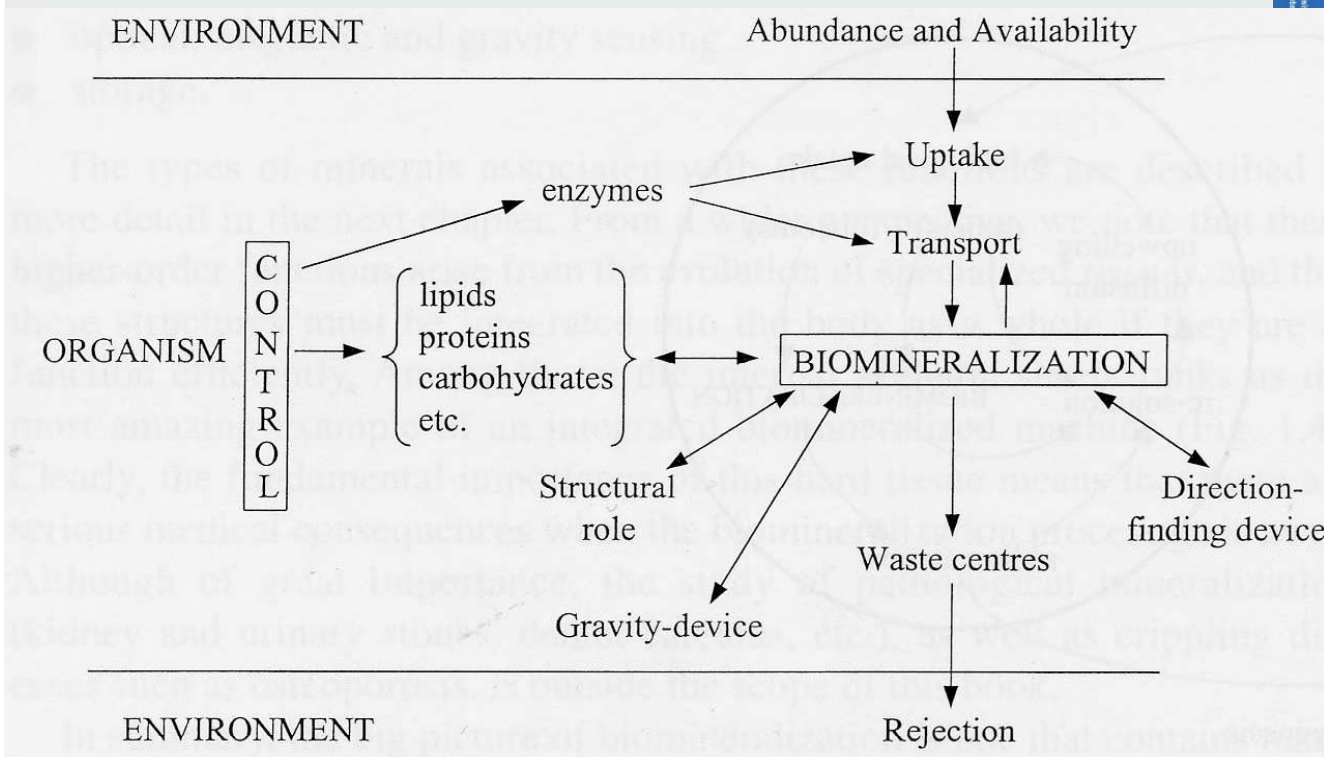


Fig. 4.30 Formation of enamel crystals. An octacalcium phosphate (OCP) precursor phase is formed within an organic envelope (OE) and then overgrown with a single crystal of hydroxyapatite (HAP). Traces of the OCP phase are left as a central dark line (CDL) inside the mature crystal.

Table 4.2 Epitaxial deposition of inorganic crystals on inorganic substrates. A positive percentage misfit value indicates that the overgrowth lattice is larger than the substrate lattice

| Substrate | Overgrowth | Lattice misfit % |
|-------------------|------------|------------------|
| PbS | Nal | 8 |
| | KCl | 5 |
| | NaBr | -1 |
| | NaCl | -6 |
| | AgBr | -4 |
| | AgCl | -7 |
| | RbBr | 7 |
| | RbCl | 3 |
| | KBr | 3 |
| | Nal | 1 |
| CaCO ₃ | KCl | -2 |
| | NaBr | -7 |
| | NaBr | 8 |
| | NaCl | 3 |
| | LiBr | 0 |
| CaF ₂ | LiCl | -6 |
| | NaBr | 6 |
| | NaCN | 6 |
| | AgBr | 3 |
| | AgCN | 3 |
| NaCl | AgCl | 1 |
| | KF | -5 |

Living System



Living System

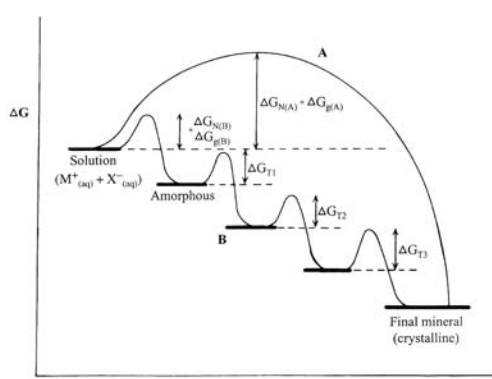
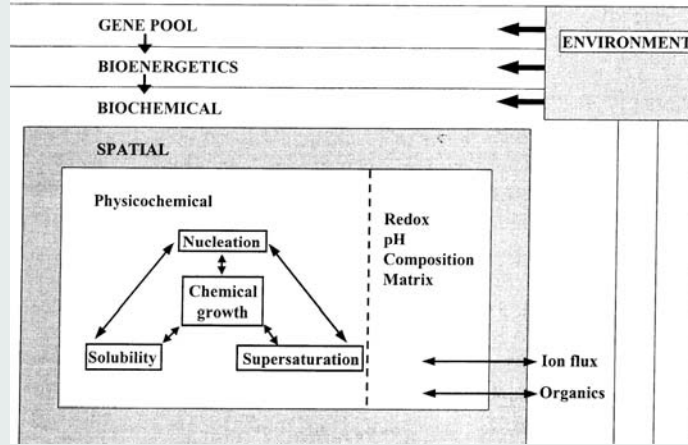


Fig. 4.25 Pathways to crystallization and polymorph selectivity: (A) direct (B) sequential. See text for details.

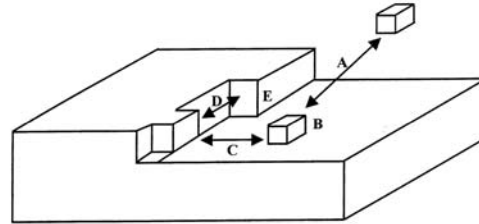


Fig. 4.6 Layer-by-layer mechanism of crystal growth. See text for details.

Biosensors



Tumor + Gene Therapy

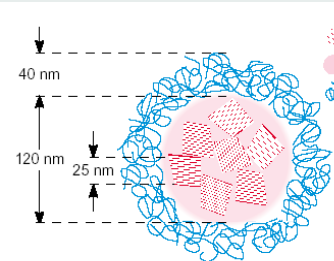


Abbildung 27. Kern-Schale-Aufbau der β -Carotin-Hydrosol-Partikel. Den spektroskopischen Daten und den Weitwinkelröntgenspektren (WAXS) zufolge besteht der Wirkstoff-Kern aus H- und J-Aggregaten mit Abmessungen bis zu 30 nm, entsprechend einer maximalen Aggregationszahl von 10000 Molekülen.

